A committed postselection precursor to natural TCRαβ+ intraepithelial lymphocytes

Christoph SN Klose[1,2,3], Jonas F Hummel[1,3], Lena Faller[1], Yannick d'Hargues[1,2], Karolina Ebert[1,2] and Yakup Tanriver[1,2]

The intestine is a major immune organ with several specialized lymphoid structures and immune cells. Among these are thymus-derived natural intraepithelial lymphocytes (IELs) that lack expression of the classical co-receptors CD4 or CD8αβ (double negative (DN)). Natural IELs are both αβ+ and γδ+ T cells that play important roles in the maintenance of the epithelial barrier at steady state and during inflammation. The transcription factor T-bet is essential for the peripheral development of natural IELs, but its role during thymic development has remained less clear. Here we show that a T-bet gradient in DN TCRαβ+NK1.1− thymocytes (IEL precursors (IELPs)) determines IEL fate in natural TCRαβ+ IELs. Employing T-bet ZsGreen reporter mice in in vitro cultures and in vivo transfer experiments, we demonstrate that with increasing expression of T-bet, DN TCRαβ+NK1.1− thymocytes are gradually restricted to a DN IEL fate. Furthermore, we show that the natural TCRαβ+ IELs seed the intestine within the first month of life. This in turn is preceded by the appearance of T-bet− and T-bet+ IELPs that egress from the thymus in a sphingosine-1-phosphate (S1P)-dependent manner. In summary, the use of T-bet reporter mice has enabled us to identify and refine an immediate and clearly committed postselection precursor of natural TCRαβ+ IELs.

INTRODUCTION

At the mucosa of the intestine, a single layer of epithelial cells separates the host tissue from the immunostimulatory content of the gut lumen such as microbes, nutrients, and metabolites. In order to maintain tolerance but still be able to mount potent immune responses, the mucosal immune system is equipped with various special immune cell types that are very rare in secondary lymphoid organs. One of these mucosa-associated immune cells are intraepithelial lymphocytes (IELs) that are interspersed at the basolateral side of epithelial cells. Here they fulfill important functions in the maintenance of the epithelial barrier by promoting cellular turnover of the epithelium, providing first-line responses against pathogens and tumors, and also regulating overt immune responses to limit collateral damage to the intestinal barrier.[1] Developmentally, two types of IELs can be distinguished. Induced IELs are the progeny of conventional CD4 and CD8αβ T cells after they have engaged their cognate antigen in the periphery, e.g., during an infection. Thus, induced IELs are rare in newborn or germ-free mice and accumulate over time in conventionally housed mice. In contrast, natural IELs are fate determined during thymic development, have an oligoclonal[2] and skewed T cell receptor (TCR) repertoire toward self,[3] and can be found in normal numbers in germ-free mice.[4] Natural IELs are composed of DN (double negative; i.e., lacking expression of CD4 or CD8αβ) γδ+ T cells as well as αβ+ T cells, with the large majority of cells expressing the homodimer CD8αα that can bind the nonclassical major histocompatibility complex, class I (MHC I) molecule thymic leukemic antigen.[5]

It has been reported that expression of the CD8αα homodimer in the thymus defines the earliest preselection precursors of IELs that in addition coexpress CD4 and CD8αβ and are therefore called triple-positive thymocytes.[6] In contrast to conventional T cells, natural TCRαβ+ IELs are generated in the thymus by interaction with high-affinity ligands presented on classical and nonclassical MHC I molecules, a process coined as agonist selection.[6] Evidently, the majority of these cells will undergo apoptosis during negative selection.[7]

Nevertheless, some cells will receive, yet unknown, survival signals, divert from clonal deletion, and further differentiate into IELs. This sequence of events is clearly supported by recent reports that have shown that the TCR specificity against self appeared to be the primary determinant of natural TCRαβ[+] IEL lineage commitment.[8,9] Postselection IEL precursors (IELPs) downregulate CD4 and CD8αβ (DN) and are now defined by expression of the rearranged TCR, upregulation of CD5 and

CD90, as well as lack of NK1.1 to exclude natural killer T (NKT) cells (DN TCRβ^{+}CD5^{+}CD90^{+}NK1.1^{−} = IELPs).[6] Subsequently, IELPs leave the thymus and migrate to the epithelium of the small intestine, a process that is guided by CCR9 and β$_7$ integrins.[10] Upon arrival in the epithelial niche, the cells downregulate CD5 and CD90 and upregulate CD103 and CD8αα, a process that is dependent on interleukin-15 (IL-15) trans-presented by intestinal epithelial cells.[11]
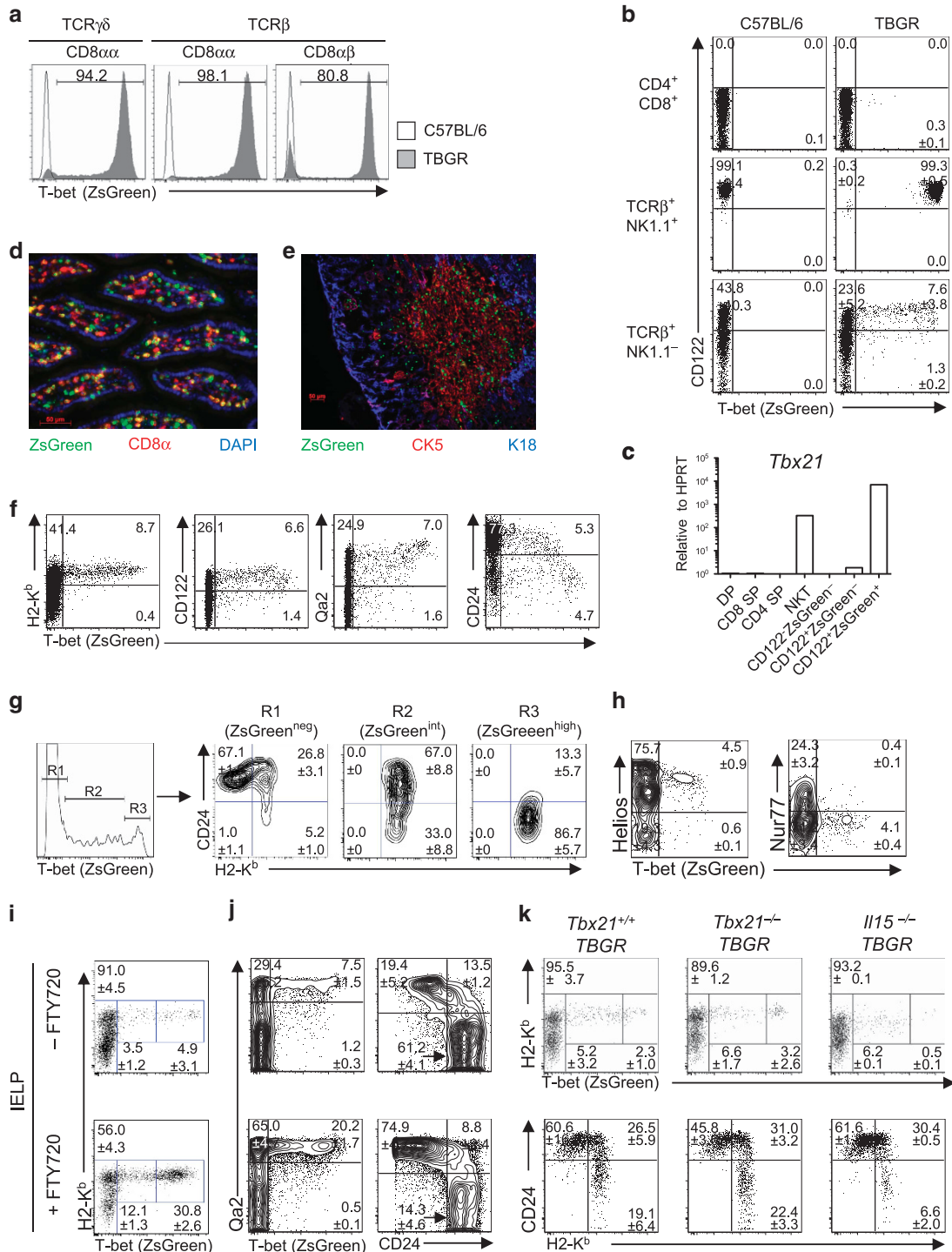
As outlined, much has been learned about the stepwise process of thymic development and the TCR specificity of natural TCRαβ[+] IELs. However, the transcriptional programs that govern these processes have just started to be explored. Recently, we[4] and others[12] have shown that the T-box transcription factor T-bet plays a nonredundant and cell-intrinsic role in the development of both TCRαβ and TCRγδ natural IELs. T-bet is not required for thymic IEL commitment but is necessary for the IL-15-driven expansion and differentiation of thymic IELPs.[4]

The common definition of thymic IELPs as DN TCRβ^{+} CD5^{+}CD90^{+}NK1.1^{−} must be treated with caution, as this would imply a homogeneous population. Intriguingly, in vivo transfer of IELPs cells gave rise to not only natural TCRαβ[+] IELs T cells but also a very sizeable number of CD8αβ^{+} T cells, arguing that these cells contain a heterogeneous population of precursors.[4,6,13] In addition, transcription factors like Egr2 or Helios, where the latter marks thymocytes with a history of strong agonist interaction, are not uniformly expressed in IELPs, further questioning the homogeneity of this population. Finally, T-bet is only expressed in a minority of Helios[+] IELPs, whereas it is expressed in virtually all natural IELs.[4] Hence, we focused on T-bet to more accurately define a population of natural IELs. We used recently developed T-bet reporter mice (Tbx21[ZsGreenTg], hereafter called TBGR mice[14]) to characterize and follow the fate of T-bet^{+} IELPs. T-bet^{+} IELPs are mature thymocytes (H2-K[b+]CD24^{−}Qa2^{high}) that egress from the thymus in a sphingosine-1-phosphate (S1P) dependent manner that can be blocked with FTY720. By crossing TBGR mice with Tbx21^{−/−} and Il15^{−/−} mice, we also demonstrate that T-bet does not regulate its own expression in IELPs and has no effect on the final maturation of H2-K[b+]CD24^{-} IELPs. In contrast, IL-15 acts at least via two mechanisms on IELPs. First, by boosting the expression of T-bet from a T-bet[intermediate (int)] to a T-bet^{high} status and, second, by guiding the maturation of H2-K[b+]CD24^{-} IELPs, that is independent of T-bet Finally, use of TBGR mice allowed us to sort T-bet^{+} IELPs to high purity. Differentiation experiments in vivo and in vitro showed a clear correlation between T-bet expression and a lack of differentiation potential into conventional CD8αβ^{+} T cells.

RESULTS

A fraction of IELPs in the thymus expresses T-bet

In order to analyze the developmental potential of thymic T-bet[+] IELPs, we wanted to make use of recently generated bacterial artificial chromosome transgenic TBGR mice.[14] It has been established that the reporter faithfully reflects T-bet expression in T helper type1 cells, but its usefulness in innate-like lymphocytes, e.g., IELs and NKT cells, has not been addressed so far. We have recently documented that IELs uniformly express the transcription factor T-bet and that T-bet is indispensable for development of CD8αα[+] TCRαβ[+] and TCR γδ^{+} T cells in the epithelium of the small intestine.[4] Using TBGR mice, we confirmed expression of ZsGreen (T-bet) in TCRαβ[+] CD8αα[+] and TCRαβ[+] CD8αβ[+] as well as TCRγδ[+] IELs by flow cytometry and immunofluorescence (see **Figure 1a,d**, for gating see **Supplementary Figure S1a** online). In the thymus, and as predicted, double-positive thymocytes lacked expression of T-bet, whereas NKT cells expressed high levels of T-bet (**Figure 1b**, for gating see **Supplementary Figure S1b**). In line with our previous results, T-bet was only expressed by a fraction of cells that meet the operative definition of IELPs ($=$DN TCRβ^{+}CD5^{+}CD90^{+}NK1.1^{−}; **Figure 1b**, for gating see **Supplementary Figure S1b**) and which in addition expressed high levels of CD122. Moreover, ZsGreen expression in flow cytometry corresponded extremely well with Tbx21 mRNA and T-bet protein expression in thymic subsets (**Figure 1c** and **Supplementary Figure S1c**). Next, we wanted to determine the thymic niche of IELPs by immunofluorescence using a similar approach. However, we were unable to establish a reliable staining for NK1.1. Nevertheless, immunofluorescence analysis of thymi from TBGR mice revealed that T-bet^{+} cells were largely localized in the cytokeratin 5 (CK5)-positive thymic medulla (**Figure 1e**) that also includes T-bet[+] NK and NKT cells. T-bet expression in IELPs correlated well with progressive development as T-bet[+] (ZsGreen) IELPs were positive for the MHC class I molecule H2-K[b], CD122, and Qa2, and partially negative for CD24 (**Figure 1f**). Detailed analysis of the coexpression of thymic maturation markers CD24 and H2-K[b] showed that T-bet expression increased with thymic development, whereby T-bet^{high} IELPs were CD24^{-}H2-K[b+] (**Figure 1f,g**).[15] The

---

Figure 1 A subset of intraepithelial lymphocyte precursors (IELPs) expresses T-bet. (**a,b**) Flow cytometry analysis of cells purified from the epithelium of the (**a**) small intestine or the (**b**) thymus of 4-week-old C57BL/6 mice or TBGR mice. Pregating is shown in **Supplementary Figure S1a,b**. Histogram data of IELs are representative of at least three independent experiments. Numbers denote percentage of cells in the gate (mean ± s.e.m., at least 3 mice per genotype for thymi). (**c**) Tbx21 mRNA expression of different flow cytometry-sorted thymocyte populations from TBGR mice analyzed by qPCR, gating strategy for ZsGreen subpopulations as shown in **b** (double positive (DP); single positive (SP)). (**d,e**) Immunofluorescent staining of sections from the (**d**) small intestine or the (**e**) thymus of TBGR mice for the indicated markers. Representative pictures taken with (**d**) $\times$ 20 or (**e**) $\times$ 10 original magnification are shown. (**f**) Flow cytometry analysis of H2-K[b], CD122, Qa2, and CD24 in relation to ZsGreen (T-bet) in IELPs from TBGR mice. (**g**) Flow cytometry analysis of thymic maturation markers CD24 and H2-K[b] in ZsGreen[−], ZsGreen[int], and ZsGreen[high] IELPs. Numbers in quadrant gates denote percentages (mean ± s.e.m.) from four analyzed TBGR mice. (**h**) Contour plot of IELPs analyzed for the expression of T-bet vs. Helios and Nur77, respectively. Numbers in quadrant gates denote percentages (mean ± s.e.m.) from four analyzed TBGR mice. (**i,j**) The 6–8-week-old TBGR mice were treated with 5 µg ml^{−1} FTY720 for 2 weeks or left untreated as a control. After treatment IELPs were analyzed for the expression of (**i**) T-bet vs. H2-K[b], (**j**) T-bet vs. Qa2, and (**j**) CD24 vs. Qa2. Numbers in quadrant gates denote percentages (mean ± s.e.m.) from at least three analyzed TBGR mice per treatment group. (**k**) Flow cytometry analysis of ZsGreen, CD24, and H2-K[b] in IELPs from wild-type TBGR, Tbx21^{−/−} TBGR, and Il15^{−/−} TBGR mice. Numbers in quadrant gates denote percentages (mean ± s.e.m.) from at least three mice per genotype.
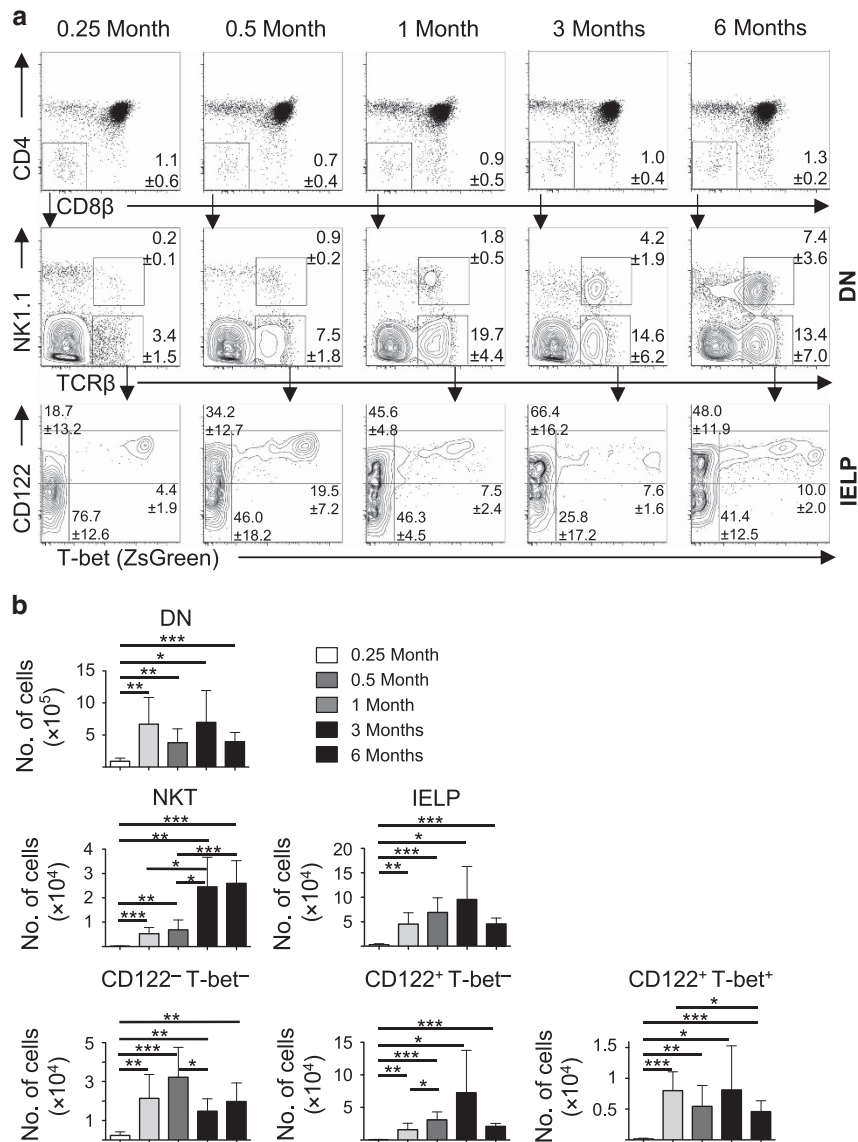
Figure 2 T-bet$^+$ intraepithelial lymphocyte precursors (IELPs) increase over the first 2 weeks of life and remain constant thereafter. (**a**) Upper row shows flow cytometric analysis of freshly isolated thymocytes from TBGR mice of different ages (0.25, 0.5, 1, 3, and 6 months). Double-negative (DN) thymocytes (CD4$^-$CD8β^-) at different ages were further analyzed for the presence of natural killer T (NKT) cells (NK1.1$^+$TCRβ^+) and IELPs (NK1.1$^-$TCRβ^+) (both middle row). In the bottom row IELPs were analyzed and divided into three subpopulations based on the expression of CD122 and T-bet (ZsGreen): CD122$^-$T-bet$^-$, CD122$^+$T-bet$^-$, and CD122$^+$T-bet$^+$. Arrows between rows indicate sequential gating strategy. Numbers in or next to quadrant gates denote percentages (mean ± s.e.m.) from at least four mice per time point. (**b**) Absolute cell numbers (mean ± s.e.m.) of DN cells (as gated in upper row of **a**), NKTs and IELPs (as gated in middle row of **a**), and CD122$^-$T-bet$^-$, CD122$^+$T-bet$^-$, and CD122$^+$T-bet$^+$ IELPs (as gated in bottom row of **a**) are given for the different cell populations and time points as described in (**a**). *$P < 0.05$; **$P < 0.01$; and ***$P < 0.001$.

superior brightness and dynamic range of ZsGreen was also largely maintained during intranuclear flow cytometry. Hence, we initially confirmed our previous data that the overwhelming majority of T-bet$^+$ IELPs are Helios$^+$ (**Figure 1h**), a marker that strongly correlates with strong agonist selection in the thymus. Intriguingly, T-bet$^+$ IELPs were negative for Nur77 (**Figure 1h**), whose expression also indicates the strength of the TCR stimulus in conventional T cells and CD4$^+$ CD25$^+$ regulatory T cells. This phenotype is however not unprecedented among agonist-selected innate-like T cells and is shared with T-bet$^+$NK1.1$^+$ iNKT cells (stage 3) that transiently upregulate Nur77 (stage 0) and

then gradually loose it during thymic development.[16] Similar to CD4 and CD8 single-positive thymocytes, ZsGreen^{high} (i.e., T-bet^{high}) IELPs egress from the thymus in a S1P-dependent manner that can be blocked by treating TBGR mice with FTY720 for 14 days (**Figure 1i,j**). As a result, ZsGreen$^{int/high}$ (T-bet$^{int/high}$) IELPs, which are as expected H2-Kb$^+$ (**Figure 1i**), Qa2^{high}, and CD24^{low} (**Figure 1j**), accumulate in the thymus after FTY720 treatment. Thymic T-bet^{high} IELPs share many similarities with TCR$\alpha\beta^+$ CD8$\alpha\beta^-$ IELs in the intestinal epithelium (see also **Figure 5**). Hence, we were wondering whether the accumulation of thymic IELPs might lead to a decreased frequency of TCR$\alpha\beta^+$ CD8$\alpha\beta^-$ IELs in the

periphery. Indeed, mice treated with FTY720 showed a tendency toward a decreased frequency of TCRαβ$^+$ CD8αβ$^-$ IELs in the intestinal epithelium (**Supplementary Figure S2a**). However, that difference did not reach statistical significance. Further analysis of intestinal TCRαβ$^+$ CD8αβ$^-$ IELs showed a significant reduction of T-bet$^-$ TCRαβ$^+$ CD8αβ$^-$ IELs after FTY720 treatment, whereas T-bet^{high} TCRαβ$^+$ CD8αβ$^-$ IELs (**Supplementary Figure S2b**) were overrepresented. This would imply that despite the accumulation of T-bet$^{int/high}$ IELPs in the thymus after FTY720 treatment, a significant proportion of IELPs leave the thymus before they express T-bet. The FTY720 experiments are in agreement with a recent report that implicated that thymic CD8αα$^+$ IELPs leave the thymus in a S1P1-dependent manner and therefore mice with a conditional knockout for *S1pr1* (encodes for S1P1) in the hematopoietic system have severely reduced numbers of TCRαβ$^+$ CD8αα$^+$ and TCRγδ$^+$ IELs.[17] In order to better understand the regulation of T-bet we crossed TBGR mice with *Tbx21*$^{-/-}$ and *Il15*$^{-/-}$ mice, respectively. *Tbx21*$^{-/-}$ TBGR mice showed no relevant reduction in ZsGreen^{high} cells (**Figure 1k**, middle column) and had normal numbers of CD24$^-$H2-K^{b+} IELPs (**Figure 1k**, middle column). Hence, T-bet neither regulates its own expression during thymic IELP development nor does it affect all stages of thymic maturation in IELPs. In contrast, *Il15*$^{-/-}$ TBGR mice showed a striking reduction in ZsGreen^{high} cells (**Figure 1k**, right column) and had a severe block in final maturation toward CD24$^-$H2-K^{b+} IELPs (**Figure 1k**, right column). Therefore, the actions of IL-15 cannot be solely explained through T-bet as *Tbx21*$^{-/-}$ TBGR mice had normal numbers of CD24$^-$H2-K^{b+} IELPs. As a result the intestinal epithelium of *Il15*$^{-/-}$ TBGR mice showed a reduction of TCRαβ$^+$ CD8αβ$^-$ IELs and these cells had significantly less T-bet than TCRαβ$^+$ CD8αβ$^-$ IELs from TBGR mice (**Supplementary Figure S2c**).

In summary, TBGR mice show a faithful expression of the reporter as a surrogate for T-bet in natural IELs and their thymic precursors and can thus be used to analyze the role of T-bet in IEL development.

Thymic ontogeny of T-bet$^+$ IELPs

It has been shown for TCRγδ$^+$ T cells that specific subsets arise during discrete time windows before or after birth in the thymus and subsequently migrate to their destined peripheral organ. As TCRαβ$^+$ CD8αα$^+$ IELs share many features with TCRγδ$^+$ CD8αα$^+$ IELs we next explored their thymic and peripheral development after birth in TBGR mice. At 1 week after birth (0.25 month), only small numbers of IELPs could be detected in the thymus. Nevertheless, a clear population of T-bet$^+$ (i.e., ZsGreen$^+$) could already be identified at this stage (**Figure 2a**, left column, and **Figure 2b**, bottom row). In the following week (0.5 month) we noticed a striking and significant increase in the percentage and absolute numbers of IELPs and T-bet$^+$ IELPs (**Figure 2a**, second column, and **Figure 2b**, bottom row) that is in agreement with the appearance of thymic IELPs in TCR transgenic mouse

strains.[15] The absolute number of T-bet$^+$ IELPs did not change significantly over the following months (**Figure 2a,b**). Intriguingly, it appeared that within the first month of life T-bet$^+$ IELPs did not reach the very high levels of T-bet that can be seen at later stages in life (compare MFI for ZsGreen in 0.25, 0.5, and 1 month vs. 3 and 6 months). However, because of high variance, that difference did not reach statistical significance. In summary, we can conclude that in contrast to some subsets of TCRγδ$^+$ T cells the absolute numbers of T-bet$^+$ IELPs increase over the first 2 weeks of life and then remain constant for the time hereafter.

Intestinal ontogeny of IELs

The intestinal appearance of natural TCRαβ$^+$ IELs followed the development of their thymic precursors. At week 1 (0.25 month), we could hardly detect any TCRαβ$^+$ CD8αα$^+$ IELs, whereas TCRαβ$^+$ CD8αβ$^+$ IELs were already present, although at low numbers (**Figure 3a,b,c**). Presumably, as a result of their thymic expansion (see **Figure 2a,b** for comparison) relevant numbers of TCRαβ$^+$ CD8αα$^+$ IELs and TCRαβ$^+$ CD8αβ$^-$ IELs became first detectable at week 2 (0.5 month). Thereafter, the number of all IEL populations increased gradually until they maintained stable numbers between 3 and 6 months. One intriguing finding at weeks 1 and 2 was the fact that these were the only time points at which the number of TCRαβ$^+$ CD8αβ$^-$ IELs was equal or even higher than the number of TCRαβ$^+$ CD8αα$^+$ IELs (**Figure 3a**, first two columns, and **Figure 3c**). At these stages, and similar to thymic IELPs, with which they share the phenotype DN TCRβ$^+$NK1.1$^-$, TCRαβ$^+$ CD8αβ$^-$ IELs do not uniformly express T-bet (**Figure 3d,e**, middle bar diagram), suggesting that they might be recent thymic emigrants (RTEs) and the precursors of TCRαβ$^+$ CD8αα$^+$ IELs; a hypothesis that we tested later in this study (see **Figure 5**). In contrast and independent of age, TCRαβ$^+$ CD8αα$^+$ IELs were virtually all T-bet$^+$ (**Figure 3d,e**, left bar diagram).

Expression of T-bet in IELPs is correlated with strongly decreased CD8αβ$^+$ T-cell differentiation potential

We hypothesized before that T-bet$^+$ IELPs are committed to an unconventional T-cell fate and lack potential to differentiate into conventional T cells. To test this hypothesis we isolated ZsGreen$^+$ (T-bet$^+$) and ZsGreen$^-$ (T-bet$^-$) IELPs by flow cytometry and differentiated these cells *in vitro* with recombinant IL-15 (**Figure 4**). The analysis of *in vitro* cultures by flow cytometry revealed that T-bet$^+$ IELPs had a markedly reduced potential to give rise to CD8αβ$^+$ T cells (**Figure 4a,b**). To further investigate the inverse correlation between T-bet expression and CD8αβ potential, we divided IELPs into four groups representing cells with no, low, intermediate, or high expression of T-bet, as judged by ZsGreen levels (for sorting strategy see **Supplementary Figure S3**). *In vitro* differentiation of IELPs with different levels of T-bet expression showed a clear inverse correlation between the expression of T-bet and differentiation potential into CD8αα$^+$ T cells (**Figure 4c,d**). In fact, T-bet^{high} IELPs had hardly any CD8αβ potential *in vitro*. Although less pronounced, there was
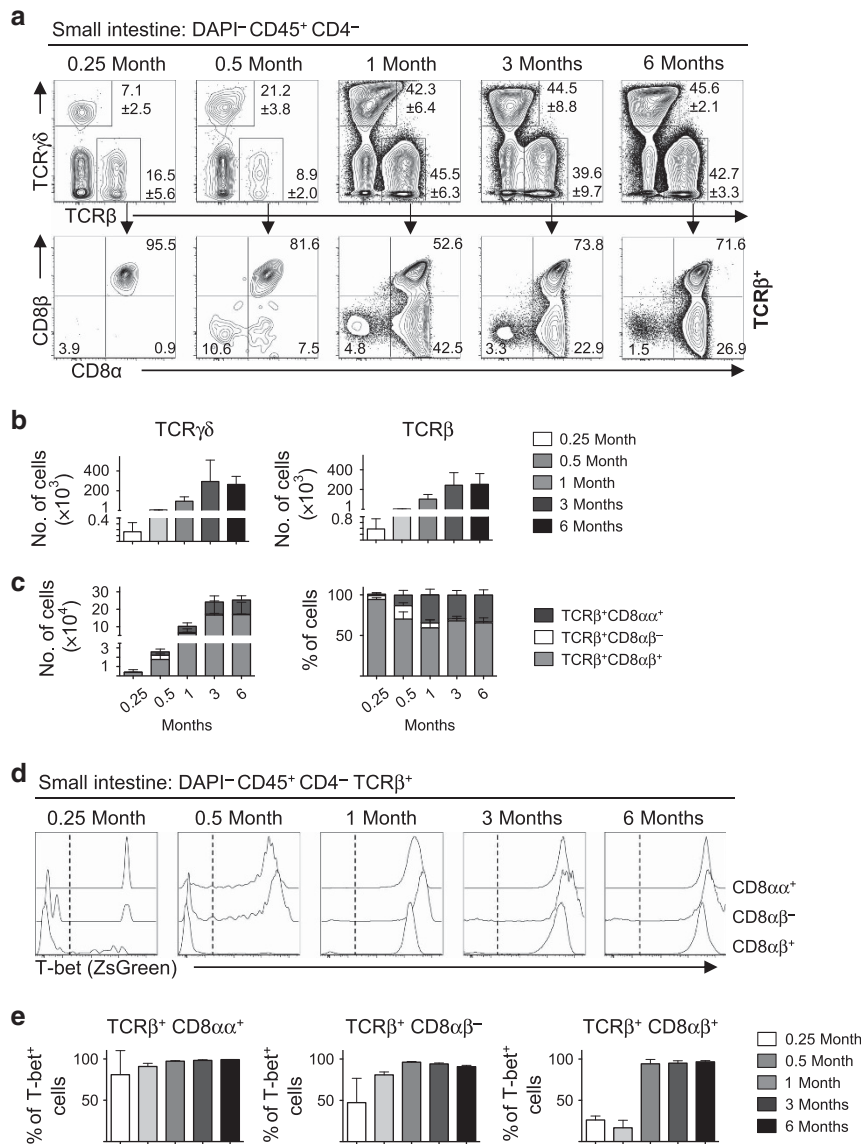
Figure 3 T-bet⁺ intraepithelial lymphocytes (IELs) increase in the small intestine during the first weeks of life and remain stable between 3 and 6 months. (**a**) Flow cytometry analysis of lymphocytes isolated from the epithelium of the small intestine of TBGR mice of different ages (0.25, 0.5, 1, 3, and 6 months). Representative dot plots in the upper row were pregated on DAPI⁻CD45⁺CD4⁻ cells and TCRβ⁺ cells (arrow) were further assessed for the expression of CD8αα and CD8αβ. Numbers in or next to quadrant gates denote percentages (mean ± s.e.m.) from at least four mice per time point. (**b**) Bar diagrams show absolute cells numbers of TCRγδ and TCRβ IELs for the different time points as shown in **a** (upper row). (**c**) Bar diagrams show absolute cells numbers (left, mean ± s.e.m.) and percentages (right, mean ± s.e.m.) of the three different TCRαβ⁺ IEL populations (CD8αβ⁻, CD8αα⁺, and CD8αβ⁺) as gated in (**a**) (lower row). (**d**) Representative histogram offsets for the comparison of T-bet (ZsGreen) expression in TCRαβ⁺ IEL subpopulations as gated in (**a**) (lower row) at different time points after birth. (**e**) Percentage of T-bet⁺ (ZsGreen⁺) cells within the three TCRαβ⁺ IEL subpopulations as gated in (**a**) (lower row) and analyzed in **d** at different time points after birth. Percentages are expressed as mean ± s.e.m. from at least four mice per time point.

also a reduced potential of T-bet^int and T-bet^high IELPs to develop into CD8αα⁺ T cells (**Figure 4c,d**). This indicates that the *in vitro* setting is not able to fully mimic the *in vivo* situation with its accessory cellular components and soluble mediators.

Although we performed extensive translational profiling by flow cytometry, we could not identify a single marker that could be used as a unique surrogate marker for all T-bet⁺ IELPs (data not shown). For example, the level of CD122 correlated well with T-bet expression in IELPs (**Figure 4e**), but CD122^high cells harbored a mixture of T-bet⁺ and T-bet⁻ IELPs (**Figure 4e**).

Hence and as predicted, *in vitro* differentiation of these latter cells also gave rise to a sizeable number of CD8αβ⁺ T cells (**Figure 4f**, lower row). Of note is that CD122⁻ IELPs have virtually no potential to blast or to develop into IELs that, therefore, are presumably cells destined for clonal deletion after negative selection (**Figure 4f**, upper row). One other interesting feature of the *in vitro* differentiation experiments was the fact that we reproducibly detected a prominent population of CD8αα⁺-expressing cells that were negative for T-bet (**Figure 4g**, lower right quadrants). This
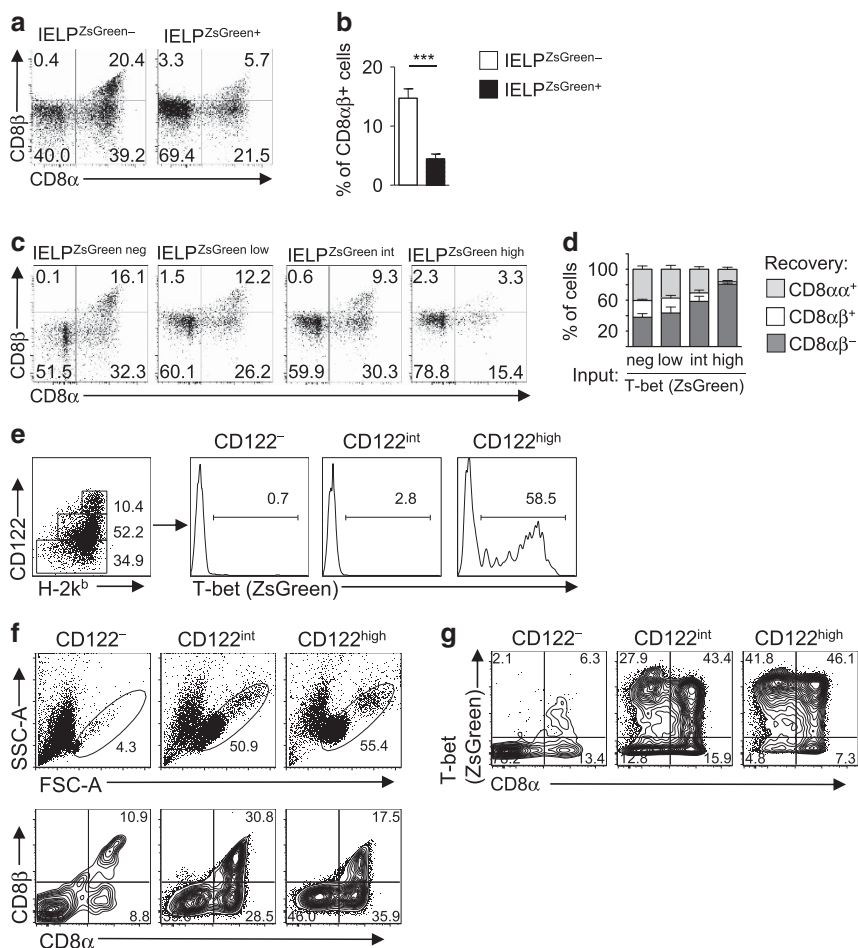
Figure 4 T-bet gradient in intraepithelial lymphocyte precursors (IELPs) inversely correlates with the potential to differentiate into conventional CD8αβ$^+$ T cells *in vivo* and *in vitro*. (**a–d**) Indicated subsets of flow cytometry sorted IELPs from TBGR mice were cultured in 200 μl complete RPMI supplemented with interleukin-15 (IL-15; 100 ng ml^{-1}) *in vitro*. Total ZsGreen$^-$ IELPs include both CD122$^+$ZsGreen$^-$ and CD122$^-$ZsGreen$^+$ IELPs. Principal gating strategy for sorting ZsGreen^{neg}, ZsGreen^{low}, ZsGreen^{int}, and ZsGreen^{high} IELPs is depicted in **Supplementary Figure S3**. (**a,c**) Dot plots show representative flow cytometry analysis for CD8α and CD8β after 7 days *in vitro* gated on DAPI$^-$CD45$^+$CD4$^-$ lymphocytes. Numbers represent percentage of cells in gates. ***$P < 0.001$. (**c,d**) Bar diagrams show percentage (mean + s.e.m., $n = 8$ (**b**) or $n = 4$ (**d**)) of CD8αβ$^-$, CD8αα$^+$, and CD8αβ$^+$ lymphocytes pooled from three independent experiments. (**e**) IELPs were divided into three subpopulations (dot blot; CD122$^-$, CD122^{int}, CD122^{high}) and the expression level of T-bet (ZsGreen) was analyzed in each population (histograms). Results are representative for at least five individual TBGR mice. (**f**) IELP subsets were flow cytometry sorted based on CD122 level as shown in (**e**) and stimulated with IL-15 (100 ng ml^{-1}) *in vitro*. At the end of the culture cells were analyzed for blasting (**f**, upper row) and the upregulation of CD8α and CD8β (**f**, lower row). (**g**) Cells as described in (**f**) were further analyzed for the coexpression of T-bet (ZsGreen) and CD8α. (**f,g**) Numbers in quadrant gates denote percentages. One representative result out of three independent experiments is shown.

would imply that some IELs first upregulate CD8αα and then T-bet. However, this pathway might be of minor relevance *in vivo* as, on average, only 2% of all CD8αα IELs in adult mice are T-bet$^-$ (**Figure 3d,e**). Hence currently, TBGR mice are ideally suited to identify and sort T-bet^{high} IELPs with a reduced CD8αβ$^+$ potential.

Next, we wanted to confirm our *in vitro* data by injecting different IELP populations from TBGR mice into alymphoid *Rag2$^{-/-}$ Il2rg$^{-/-}$* mice (**Figure 5**). Cells from spleen and intestinal epithelium of *Rag2$^{-/-}$ Il2rg$^{-/-}$* mice were recovered at least 4 weeks after adoptive transfer. In both organs, the potential of adoptively transferred precursors to develop into TCRαβ$^+$ CD8αβ$^+$ T cells was significantly decreased in mice that had received T-bet$^+$ IELPs compared

with mice that had been injected with T-bet$^-$ IELPs (**Figure 5a, b**). Sorting and transferring IELPs based on graded T-bet expression (for sorting strategy see **Supplementary Figure S3** online) *in vivo* confirmed that increased T-bet expression drastically reduces the potential to differentiate TCRαβ$^+$ CD8αβ$^+$ T cells in the epithelium and spleen of *Rag2$^{-/-}$ Il2rg$^{-/-}$* mice (**Figure 5c,d**). Notably, T-bet^{high} IELPs lacked any differentiation potential for CD8αβ$^+$ T cells, indicating that these cells are fully restricted to an unconventional T-cell fate (**Figure 5c,d**). As T-bet$^-$ (ZsGreen$^-$) IELP also gave rise to large numbers of CD8αα$^-$ and CD8αβ$^-$ IELs (**Figure 5a**, upper row, left dot blot), it is most likely that T-bet$^-$ IELPs harbor a subpopulation that develops into T-bet$^+$ IELPs.
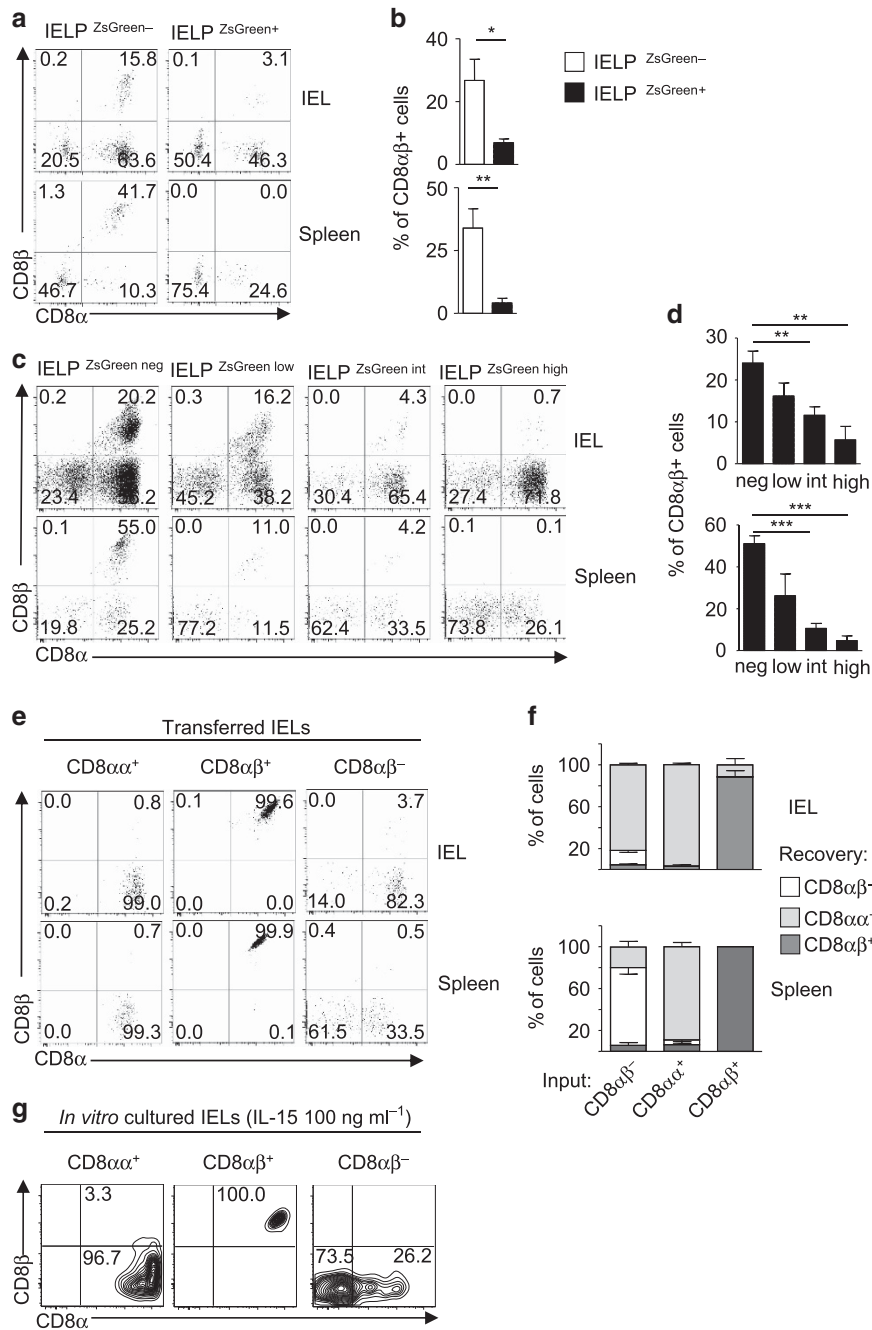
Figure 5 TCRαβ[+] CD8αβ[−] intraepithelial lymphocytes (IELs) upregulate CD8αα *in vivo* and *in vitro*. (**a–d**) Indicated subsets of flow cytometry sorted IEL precursors (IELPs) were injected into BALB/c *Rag2*^{−/−} *Il2rg*^{−/−} mice (H-2[d]). (**a,c**) Cells were purified from the spleen or the epithelium of the small intestine of *Rag2*^{−/−} *Il2rg*^{−/−} mice and analyzed by flow cytometry for CD8α and CD8β. Plots were electronically pregated on H2-K[b+]CD45^{+}CD4^{-}TCRβ^{+} T-bet^{+} (ZsGreen^{+}) lymphocytes. (**b,d**) Bar diagrams show percentage (mean + s.e.m., $n = 8$–9 (**b**) or $n = 4$–5 (**d**)) of CD8αβ[+] lymphocytes from spleen or small intestine pooled from three independent experiments. *$P < 0.05$; **$P < 0.01$; and ***$P < 0.001$. (**e**) Indicated subsets of flow cytometry sorted TCRαβ[+] IELs from TBGR mice were injected into *Rag2*^{−/−} *Il2rg*^{−/−} mice. Cells were purified from the epithelium of the small intestine or the spleen of *Rag2*^{−/−} *Il2rg*^{−/−} mice 4–8 weeks after transfer and analyzed by flow cytometry for CD8α and CD8β. Plots are pregated on H2-K[b+]CD45^{+}CD4^{−}TCRβ^{+} T-bet ZsGreen^{+} lymphocytes. Numbers represent percentage of cells in gates. Data are representative of four independent experiments. (**f**) Percentage (mean ± s.e.m., $n = 6$–10) of recovered cells pooled from four independent experiments as described in (**e**). (**g**) Indicated subsets of flow cytometry sorted TCRαβ[+] IELs were cultured in 200 μl complete RPMI supplemented with IL-15 (100 ng ml^{−1}) *in vitro* for 4 days and analyzed for the expression of CD8α and CD8β. Plots are pregated on DAPI^{−} CD3^{+} cells, experiments were performed three times, and one representative result is shown.

TCRαβ^{+} CD8αβ^{−} IELs differentiate in CD8αα^{+} but not CD8αβ[+] in IELs

The differentiation experiments in the previous sections showed that, depending on the organ milieu, T-bet[+] IELPs generated significant numbers of intestinal TCRαβ[+] CD8αβ[−] IELs that lack CD8αα[+] homodimer expression. Therefore, we hypothesized that TCRαβ[+] CD8αβ[−] IELs are the precursors of CD8αα[+] IELs and that they constitute one lineage. In order

to test this hypothesis, we sorted mature TCRαβ$^+$ CD8αα$^+$, CD8αβ$^+$, and CD8αβ$^-$ IELs from the epithelium of the small intestine and adoptively transferred them into $Rag2^{-/-}$ $Il2rg^{-/-}$ mice. Flow cytometry analysis confirmed that CD8αα$^+$ and CD8αβ$^+$ are stable lineages and maintained their expression phenotype in the intestinal epithelium and the spleen (**Figure 5e,f**). In contrast, the large majority of TCRαβ$^+$ CD8αβ$^-$ IELs upregulated CD8αα$^+$ in the epithelium, whereas in the spleen the majority of transferred TCRαβ$^+$ CD8αβ$^-$ IELs remained CD8αα$^-$ (**Figure 5e,f**). The cells that upregulated CD8αα in the spleen did so at a lower level than cells that upregulated CD8αα in the intestinal epithelium (see mean fluorescence intensity for comparison in **Figure 5e**, right column). Epithelial cell-derived IL-15 is essential for the homeostasis of CD8αα$^+$ IELs. In order to test the hypothesis that the transition from TCRαβ$^+$ CD8αβ$^-$ IELs to CD8αα$^+$ IELs depends on IL-15, we sorted TCRαβ$^+$ CD8αα$^+$, CD8αβ$^+$ and CD8αβ$^-$ IELs from the epithelium of the small intestine and stimulated them *in vitro* with or without IL-15 for 4 days. All IELs were completely dependent on IL-15 during the culture period, as we did not recover any viable cells without IL-15 supplementation (data not shown). Again, we confirmed that CD8αα$^+$ and CD8αβ$^+$ are stable lineages that maintain their expression phenotype. Furthermore, we could confirm that IL-15 is able to induce the expression of CD8αα on TCRαβ$^+$ CD8αβ$^-$ IELs (**Figure 5g**, right contour blot). However, we did not obtain the high levels of CD8αα that can be seen in *ex vivo* TCRαβ$^+$ CD8αα$^+$ IELs (**Figure 5g**, left contour blot), implicating that beside IL-15 other epithelium-derived signals are necessary for the full induction of CD8αα on TCRαβ$^+$ CD8αβ$^-$ IELs.

In summary, these data clearly show that TCRαβ$^+$ CD8αα$^+$ and CD8αβ$^+$ IELs are stable terminally differentiated IEL lineages but that TCRαβ$^+$ CD8αβ$^-$ IELs are the precursors of TCRαβ$^+$ CD8αα$^+$ IELs and that their intestinal development is enforced by IL-15 and an appropriate organ milieu.

DISCUSSION

In this study we used bright fluorescent reporter mice for the transcription factor T-bet in order to get unprecedented access to the analysis of T-bet$^+$ IELPs. Expression of T-bet in a subpopulation of IELPs has been appreciated before[4] by antibody staining but usage of TBGR mice with its unique brightness and dynamic range allowed for the first time to determine the developmental potential of these cells *in vitro* and *in vivo*. In fact, we show here that the expression level of T-bet$^+$ in thymic IELPs identifies *bona fide* postselection IELPs at their penultimate step and that IELPs egress from the thymus in a S1P-dependent manner. Eventually, these cells develop into T-bet$^+$ TCRαβ$^+$ CD8αα$^+$ natural IELs in the intestine. We further unraveled that epithelial TCRαβ$^+$ CD8αβ$^-$ natural IELs are at an intermediate stage of development and represent the direct peripheral precursor of terminally differentiated T-bet$^+$ TCRαβ$^+$ CD8αα$^+$ natural IELs (**Figures 5 and 6**).

The FTY720 experiments clearly show that the IELP egresses from the thymus in an S1P-dependent manner. However, FTY720 experiments are not ideal to identify the precise developmental stage at which T cells egress from the thymus. Hence, although the treatment leads to the accumulation of T-bet^{high}CD122$^+$H2-K^{b+}Qa2^{high}CD24^{low} cells, it does not necessarily imply that IELPs leave the thymus at such maturity. Only the use of reporter mice for Rag1 (ref. 18) or Rag2 (ref. 19) allows the faithful identification of RTEs in the periphery and thus the presumable stage at which T cell leave the thymus. Analyses of these reporter mice have demonstrated that the majority of conventional CD4 and CD8 T cells leave the thymus at an immature stage (Qa2^{low}CD24^{high}).[19] Nevertheless, inhibiting thymic egress with drugs or genetic knockouts results in the accumulation of mature CD4 and CD8 T cells (Qa2^{high}CD24^{low}).[20] This discrepancy can best be explained by a model in which immature cells that cannot leave the thymus accumulate and further mature within the thymic microenvironment. Hence, it is possible that IELPs also leave the thymus at an early stage, possibly even before they express high levels of T-bet. This is supported by the analysis of the TCRαβ$^+$ CD8αβ$^-$ IEL compartment of FTY720-treated mice that shows a significant reduction in T-bet$^-$ cells (note that these cells are Qa2^{high}) that could therefore be RTEs in untreated TBGR mice (**Supplementary Figure S2b**). This would also be in line with the high percentage of T-bet$^-$ TCRαβ$^+$ CD8αβ$^-$ IELs (**Figure 3d**) in the first weeks of life, as this is the time window with the highest frequency of RTEs in the periphery.[19] However and as outlined, to formally address the hypothesis that T-bet$^{-/int}$ TCRαβ$^+$ CD8αβ$^-$ IELs are RTEs will require the use of Rag1 or Rag2 reporter mice in the future.

Similar to natural IELs, other distinct T-cell subsets such as CD1d-restricted NKT cells and regulatory T cells depend on strong agonist interaction and store-operated calcium entry for their lineage commitment.[21] Presumably, TCR-triggered release of store-operated calcium acts via calcineurin-dependent nuclear translocation of dephosphorylated NFAT1–4 (nuclear factor of activated T-cells 1–4) proteins. Next, NFAT proteins induce the expression of their target genes either on their own or by cooperation with other transcription factors.[22] For example, the transcription factors early growth response-2 and -3 (Egr2 and Egr3) are known target genes of NFAT proteins,[22,23] and it has been shown recently that Egr2 plays a nonredundant role in the development of NKT cells.[24,25] So far, the role of Egrs in CD8αα IEL development has not been addressed. The requirement for Egr2 in NKT cells is best explained by their ability to induce the expression of CD122 via binding to its promoter.[25] CD122 is necessary for IL-15 signaling that regulates both NKT and CD8αα IEL development. As a result CD122$^-$ IELPs completely fail to properly respond to IL-15 in our culture system (**Figure 4f,g**). Together with a recent report[4] we have shown here that a majority of IELPs (DN NK1.1$^-$ TCRβ$^+$) express CD122 and Egr2. T-bet, another important regulator of CD122 in the thymus, is not expressed until later stages and correlates inversely with Egr2 expression. Moreover, we show here that IL-15 acts upstream of

	Thymus						Small intestine	
TCRβ	+	+	+	+	+	+	+	+
CD24	+	+	+	+/−	−	−	−	−
H2-K	−	+	+	+	+	+	+	+
Qa2	−	−	+	+	+	+	+	+
CD122	−	−	+	+	+	+	+	+
T-bet	−	−	−	+	+	+	+	+
CD8αα	−	−	−	−	−	−	−	+

S1P

Figure 6 Schematic depiction of phenotypic changes during CD8αα TCRαβ[+] intraepithelial lymphocyte (IEL) development. Table shows chronological overview of characteristic maker expression during IEL development from thymus to intestine. The plus (+) symbol indicates expression of protein and a minus (−) symbol indicates no expression. S1P, sphingosine-1-phosphate.

T-bet (**Figure 1k**). It is therefore conceivable that Egr2 is necessary for initial IL-15 responsiveness of IELPs that is later maintained through the action of T-bet on CD122 expression. Hence, we speculate that similar to NKT cells, Egr2 plays a nonredundant role at least during the early stages of IELP development. Importantly, we could also show here that IL-15 not only acts via T-bet, but partially regulates the thymic development of IELPs independent of T-bet. It is crucial to note that despite the strong thymic phenotype of IELPs in $Il15^{-/-}$ TBGR mice, we do not believe that thymic IL-15 is quintessential for CD8αα[+] IEL development. Instead, it is intestinal IL-15 (ref. 26) that has to be presented by epithelial cells.[27] The pivotal role of the intestinal epithelial cells for the development of CD8αα[+] IELs has been further corroborated by the fact that the transgenic presentation of IL-15 in epithelial cells can rescue the development of CD8αα[+] IELs in $Il15ra^{-/-}$ mice.[11] Hence, independent of thymic IL-15, IELPs can survive, migrate to the epithelium, and differentiate into CD8αα[+] IELs, even if the intestinal epithelium is the sole source of IL-15. In the future, it will be important to compare $Tbx21^{-/-}$ TBGR and $Il15^{-/-}$ TBGR mice side by side in order to decipher the individual contributions of IL-15 and T-bet for IEL development.

As mentioned, NFAT proteins also act by cooperating with other transcription factors. Of particular interest here is the interaction between the myocyte enhancer factor-2D (MEF2D) and NFAT1.[28] This complex jointly transactivates the immediate-early gene *Nur77*, which identifies thymocytes that received a strong TCR stimulus, e.g., regulatory T cells and NKT cells. Hence, it might be counterintuitive at first that T-bet[+] IELPs stop expressing Nur77 (**Figure 1k**). However, it must be noted that NKT cells only show strong Nur77 expression at stage 0 in the thymus that then, together with Egr2,

declines.[16,25] In contrast, regulatory T cells show a constant expression of Nur77 in the thymus and the periphery.[16] It could be argued that this is due to the fact that the presentation of the selecting ligand for NKT cells is spatially and temporally tightly regulated. As the selecting ligands for CD8αα IELs are, presumably, ubiquitously expressed MHC class I-restricted self-antigens, this would rather imply that agonist-selected innate-like T cells (i.e., NKT cell, CD8αα[+] IELs) have an, for yet unknown reasons, active mechanism to shut down extended Nur77 and Egr2 expression after initial agonist selection and studies are under way to test this notion.

The transcriptional circuits that regulate the development of natural IELs have just begun to be delineated. With the aid of TBGR mice, anatomic location, and surface markers, we are now able to identify three sequential stages of natural IEL development after selection. In the future this will allow us to generate a dynamic molecular framework of natural IEL development, advance our understanding of natural IEL biology, and provide a new starting point to harness the potency of natural IELs to ameliorate intestinal immunopathology.

METHODS

Mouse strains. C57BL/6 mice were purchased from Janvier Laboratories, Le Genest-Saint-Isle, France. $Tbx21^{ZsGreenTg}$ (ref. 14) (TBGR mice), $Tbx21^{-/-}$ (ref. 29), $Il15^{-/-}$ (ref. 30) on a C57BL/6 background, and $Rag2^{-/-} Il2rg^{-/-}$ on a BALB/c background were bred locally. Animals were between 6 and 16 weeks of age if not otherwise indicated. All animal experiments were approved and are in accordance with the local animal care committees.

Isolation of IELs, thymocytes, or splenocytes. Isolation of IELs was carried out as previously described.[4] In brief, small intestine was removed, cleaned from remaining fat tissue, and Peyer's patches were identified and eliminated. Small intestine was opened longitudinally

with a scissor and washed in ice-cold phosphate-buffered saline (PBS). Dissociation of epithelial cells was performed by incubation at 37 °C in Hanks' balanced salt solution containing 5 mM EDTA or 1 mM dithiothreitol and 10 mM Hepes twice for 20 min and mechanical force with the vortexer after each incubation step. Leukocytes were further enriched by Percoll (Sigma-Aldrich, Munich, Germany) gradient centrifugation. For isolation of IELs for transfer experiments or *in vitro* differentiation, 6–8 small intestines were pooled and labeled with 4',6-diamidino-2-phenylindole (DAPI), anti-CD45.2, anti-CD4, TCRγδ, anti-TCR-β, anti-CD8α, and anti-CD8β to sort the three IEL populations DAPI⁻ CD45⁺ CD4⁻ TCRαβ⁺ CD8αβ⁻, CD8αα⁺, and CD8αβ⁺, respectively. Thymus was removed and mashed through a 70 µm cell strainer (BD Biosciences, Heidelberg, Germany) with 10 ml of PBS. After centrifugation, erythrocytes were removed through incubation in red cell lysis buffer. For isolation of IELPs for transfer experiments or *in vitro* differentiation, 6–8 thymi were pooled and the majority of double- and single-positive thymocytes were depleted by incubation with purified rat anti-CD4 (GK1.5) and anti-CD8β (YTS156.7.7) antibody (both from Biolegend, San Diego, CA), followed by anti-rat Dynabeads (Life Technologies, Carlsbad, CA) according to the manufacturer's protocol. For verification of efficient negative selection, gating, and sorting of viable thymic IELPs (DAPI⁻ CD45.2⁺ CD4⁻ CD8β⁻ NK1.1⁻ TCRβ⁺), remaining cells were labeled with anti-CD45.2, anti-CD4 (clone RM4-4, does not compete with GK1.5), anti-CD8α, anti-TCRβ, anti-NK1.1, and DAPI. For isolation of splenocytes, individual spleens from BALB/c *Rag2⁻/⁻ Il2rg⁻/⁻* mice were removed and mashed through a 70 µm cell strainer (BD Biosciences) with 10 ml of PBS. After centrifugation, erythrocytes were removed through brief incubation in red cell lysis buffer.

FTY720 treatment. The 6–8-week-old TBGR mice received drinking water *ad libitum* supplemented with 5 µg ml⁻¹ FTY720 (Cayman, Ann Arbor, MI) and 1% glucose (Sigma-Aldrich) for 2 weeks. Water was changed every other day. Control TBGR mice received water supplemented with 1% glucose. After 2 weeks, mice were killed and thymocytes and IELs isolated as described above.

Cell sorting and *in vivo* and *in vitro* differentiation. Single-cell suspension of the indicated organs were stained with fluorescent-label coupled antibodies in PBS (Ca²⁺- and Mg²⁺-free) supplemented with 2 mM EDTA and 1% bovine serum albumin (Sigma-Aldrich) and then sorted (purity > 98%) by using a BD FACSAria III cell sorter (BD Biosciences). For adoptive transfer experiments, and depending on recovery, 15–100 × 10³ thymic IELPs or 20–50 × 10³ intestinal IELs (cell preparation see above) were adoptively transferred into BALB/c *Rag2⁻/⁻ Il2rg⁻/⁻* mice for *in vivo* differentiation and mice were killed and analyzed 4–8 weeks after transfer. For *in vitro* differentiation, 5–20 × 10³ thymic IELPs or IELs (cell preparation see above) were cultured in 200 µl RPMI supplemented with 10% fetal calf serum, 10 mM Hepes, 80 µM 2-mercaptoethanol, 8 mg ml⁻¹ glutamine, 100 U ml⁻¹ penicillin, 100 µg ml⁻¹ streptomycin, and IL-15 (100 ng ml⁻¹) (PeproTech, Hamburg, Germany) in 96-well microtiter plates for 4 or 7 days.

Flow cytometry analysis. After purification, single-cell suspensions were incubated on ice with CD16/CD32 blocking antibody in order to saturate Fc receptors. All antibodies used for staining were from Biolegend unless stated otherwise. Single-cell suspensions were incubated with biotin or fluorescent-label coupled antibodies sequentially in PBS (Ca2⁺- and Mg2⁺-free) supplemented with 2 mM EDTA and 2% fetal calf serum. The following conjugated antibodies were used: CD4 (GK1.5 and RM4-4), CD45.2 (104), CD8α (53-6.7), H2-Kᵇ (AF6-88.5), TCRγδ (GL3), TCRβ (H57 − 597), CD8β (YTS156.7.7), NK1.1 (PK136), CD122 (TM-β1), CD5 (53-7.3), and rat IgG2a isotype control (RTIK2758). T-bet (4B10), Nur77 (12.14, eBioscience, Fisher Scientific GmbH, Schwerte, Germany), and Helios (22F6) were stained using the Foxp3 transcription factor staining buffer set (eBioscience). All flow cytometry experiments were acquired

using a FACS Fortessa flow cytometer and the FACS Diva software (BD Biosciences) and analyzed with FlowJo V8.8 software (FlowJo, LLC, Ashland, OR).

Immunofluorescence. Small intestine or thymus was removed cleaned by washing in ice-cold PBS and small intestine opened longitudinally. A piece of the tissue was fixed in 4% paraformaldehyde on ice for 2 h. Afterward the tissue was washed in ice-cold PBS before rehydrating the tissue in 30% (w/v) sucrose phosphate buffer overnight. Tissues samples were embedded in O.C.T. Compound (Tissue-Tek, Sakura Finetek Germany GmbH, Staufen, Germany) and snap-frozen in liquid nitrogen. Cryostat sections of 8 µm thickness were collected on frosted glass slides and dried at 37 °C for 3 h. Slides were rehydrated in PBS and blocked with 10% bovine serum albumin (Sigma-Aldrich). Small intestine samples were incubated with phycoerythrin-conjugated anti-CD8α (clone 53-6.7 Biolegend). Thymic samples were first incubated with rabbit anti-cytokeratin 5 (1:500, clone PRB-160P, gift from T. Boehm) and biotinylated mouse anti-K18 (1:100, clone Ks18.04, gift from T. Boehm, Freiburg, Germany) followed by donkey anti-rabbit Cy3 (1:500, Jackson ImmunoResearch, Suffolk, UK) and streptavidin-Alexa-647 (1:500, Biolegend). Slides were mounted with mounting medium (PermaFlour, Thermo Scientific, Waltham, MA) and each section was visually inspected. Images of representative sections were captured under a Axioplan 2 fluorescence microscope at × 20 (small intestine) or × 10 (thymus) magnification using an AxioCam camera and Axiovision LE software (all Axio devices were from Zeiss, Oberkochen, Germany).

Statistical analysis. *P* value of data sets was determined by unpaired two-tailed Student's *t*-test with 95% confidence interval. All statistical tests were performed with Graph Pad Prism V4 software (San Diego, CA) (*$P < 0.05$; **$P < 0.01$; and ***$P < 0.001$; n.s., not significant).

AUTHOR CONTRIBUTIONS
C.S.N.K and J.F.H. carried out most experiments and analyzed most of the data. L.F. generated ontogeny data and contributed to the knockouts. Y.d'H. performed immunofluorescent staining. K.E. helped with *in vitro* cell cultures. Y.T. conceived the project, directed the research, and wrote the manuscript with input from all co-authors.

DISCLOSURE
The author declared no conflict of interest.

REFERENCES
1. Cheroutre, H., Lambolez, F. & Mucida, D. The light and dark sides of intestinal intraepithelial lymphocytes. *Nat. Rev. Immunol.* **11**, 445–456 (2011).
2. Regnault, A., Cumano, A., Vassalli, P., Guy-Grand, D. & Kourilsky, P. Oligoclonal repertoire of the CD8 alpha alpha and the CD8 alpha beta TCR-alpha/beta murine intestinal intraepithelial T lymphocytes: evidence for the random emergence of T cells. *J. Exp. Med.* **180**, 1345–1358 (1994).

3. Leishman, A.J. *et al.* Precursors of functional MHC class I- or class II-restricted CD8alphaalpha(+) T cells are positively selected in the thymus by agonist self-peptides. *Immunity* **16**, 355–364 (2002).

4. Klose, C.S. *et al.* The transcription factor T-bet is induced by IL-15 and thymic agonist selection and controls CD8alphaalpha(+) intraepithelial lymphocyte development. *Immunity* **41**, 230–243 (2014).

5. Leishman, A.J. *et al.* T cell responses modulated through interaction between CD8alphaalpha and the nonclassical MHC class I molecule, TL. *Science* **294**, 1936–1939 (2001).

6. Gangadharan, D., Lambolez, F., Attinger, A., Wang-Zhu, Y., Sullivan, B.A. & Cheroutre, H. Identification of pre- and postselection TCRalphabeta+ intraepithelial lymphocyte precursors in the thymus. *Immunity* **25**, 631–641 (2006).

7. Pobezinsky, L.A. *et al.* Clonal deletion and the fate of autoreactive thymocytes that survive negative selection. *Nat. Immunol.* **13**, 569–578 (2012).

8. Mayans, S. *et al.* alphabetaT cell receptors expressed by CD4(-)CD8alphabeta(-) intraepithelial T cells drive their fate into a unique lineage with unusual MHC reactivities. *Immunity* **41**, 207–218 (2014).

9. McDonald, B.D., Bunker, J.J., Ishizuka, I.E., Jabri, B. & Bendelac, A. Elevated T cell receptor signaling identifies a thymic precursor to the TCRalphabeta(+)CD4(-)CD8beta(-) intraepithelial lymphocyte lineage. *Immunity* **41**, 219–229 (2014).

10. Wurbel, M.A. *et al.* Mice lacking the CCR9 CC-chemokine receptor show a mild impairment of early T- and B-cell development and a reduction in T-cell receptor gammadelta(+) gut intraepithelial lymphocytes. *Blood* **98**, 2626–2632 (2001).

11. Ma, L.J., Acero, L.F., Zal, T. & Schluns, K.S. Trans-presentation of IL-15 by intestinal epithelial cells drives development of CD8alphaalpha IELs. *J. Immunol.* **183**, 1044–1054 (2009).

12. Reis, B.S., Hoytema van Konijnenburg, D.P., Grivennikov, S.I. & Mucida, D. Transcription factor T-bet regulates intraepithelial lymphocyte functional maturation. *Immunity* **41**, 244–256 (2014).

13. Guo, X., Tanaka, Y. & Kondo, M. Thymic precursors of TCRalphabeta(+) CD8alphaalpha(+) intraepithelial lymphocytes are negative for CD103. *Immunol. Lett.* **163**, 40–48 (2015).

14. Zhu, J. *et al.* The transcription factor T-bet is induced by multiple pathways and prevents an endogenous Th2 cell program during Th1 cell responses. *Immunity* **37**, 660–673 (2012).

15. Yamagata, T., Mathis, D. & Benoist, C. Self-reactivity in thymic double-positive cells commits cells to a CD8 alpha alpha lineage with characteristics of innate immune cells. *Nat. Immunol.* **5**, 597–605 (2004).

16. Moran, A.E. *et al.* T cell receptor signal strength in Treg and iNKT cell development demonstrated by a novel fluorescent reporter mouse. *J. Exp. Med.* **208**, 1279–1289 (2011).

17. Odumade, O.A., Weinreich, M.A., Jameson, S.C. & Hogquist, K.A. Kruppel-like factor 2 regulates trafficking and homeostasis of gammadelta T cells. *J. Immunol.* **184**, 6060–6066 (2010).

18. Kuwata, N., Igarashi, H., Ohmura, T., Aizawa, S. & Sakaguchi, N. Cutting edge: absence of expression of RAG1 in peritoneal B-1 cells detected by knocking into RAG1 locus with green fluorescent protein gene. *J. Immunol.* **163**, 6355–6359 (1999).

19. Boursalian, T.E., Golob, J., Soper, D.M., Cooper, C.J. & Fink, P.J. Continued maturation of thymic emigrants in the periphery. *Nat. Immunol.* **5**, 418–425 (2004).

20. Matloubian, M. *et al.* Lymphocyte egress from thymus and peripheral lymphoid organs is dependent on S1P receptor 1. *Nature* **427**, 355–360 (2004).

21. Oh-Hora, M. *et al.* Agonist-selected T cell development requires strong T cell receptor signaling and store-operated calcium entry. *Immunity* **38**, 881–895 (2013).

22. Mognol, G.P., Carneiro, F.R., Robbs, B.K., Faget, D.V. & Viola, J.P. Cell cycle and apoptosis regulation by NFAT transcription factors: new roles for an old player. *Cell Death Dis.* **7**, e2199 (2016).

23. Rengarajan, J. *et al.* Sequential involvement of NFAT and Egr transcription factors in FasL regulation. *Immunity* **12**, 293–300 (2000).

24. Lazarevic, V. *et al.* The gene encoding early growth response 2, a target of the transcription factor NFAT, is required for the development and maturation of natural killer T cells. *Nat. Immunol.* **10**, 306–313 (2009).

25. Seiler, M.P. *et al.* Elevated and sustained expression of the transcription factors Egr1 and Egr2 controls NKT lineage differentiation in response to TCR signaling. *Nat. Immunol.* **13**, 264–271 (2012).

26. Schluns, K.S., Nowak, E.C., Cabrera-Hernandez, A., Puddington, L., Lefrancois, L. & Aguila, H.L. Distinct cell types control lymphoid subset development by means of IL-15 and IL-15 receptor alpha expression. *Proc. Natl. Acad. Sci. USA* **101**, 5616–5621 (2004).

27. Mortier, E. *et al.* Macrophage- and dendritic-cell-derived interleukin-15 receptor alpha supports homeostasis of distinct CD8+ T cell subsets. *Immunity* **31**, 811–822 (2009).

28. Blaeser, F., Ho, N., Prywes, R. & Chatila, T.A. Ca(2+)-dependent gene expression mediated by MEF2 transcription factors. *J. Biol. Chem.* **275**, 197–209 (2000).

29. Szabo, S.J., Sullivan, B.M., Stemmann, C., Satoskar, A.R., Sleckman, B.P. & Glimcher, L.H. Distinct effects of T-bet in TH1 lineage commitment and IFN-gamma production in CD4 and CD8 T cells. *Science* **295**, 338–342 (2002).

30. Kennedy, M.K. *et al.* Reversible defects in natural killer and memory CD8 T cell lineages in interleukin 15-deficient mice. *J. Exp. Med.* **191**, 771–780 (2000).